Published online January 12, 2005

260–271 *Nucleic Acids Research, 2005, Vol. 33, No. 1*
doi:10.1093/nar/gki165

Processing of a complex multiply damaged DNA site by human cell extracts and purified repair proteins

Grégory Eot-Houllier, Séverine Eon-Marchais, Didier Gasparutto[1] and Evelyne Sage*

CNRS-IC UMR 2027, Institut Curie, Centre Universitaire, Bât. 110, F-91405 Orsay, France and
[1]Laboratoire 'Lésions des Acides Nucléiques', Service de Chimie Inorganique et Biologique, Département de Recherche Fondamentale sur la Matière Condensée, CEA-Grenoble, F-38054 Grenoble Cedex 9, France

Received September 27, 2004; Revised and Accepted December 15, 2004

ABSTRACT

Clustered DNA lesions, possibly induced by ionizing radiation, constitute a trial for repair processes. Indeed, recent studies suggest that repair of such lesions may be compromised, potentially leading to the formation of lethal double-strand breaks (DSBs). A complex multiply damaged site (MDS) composed of 8-oxoguanine and 8-oxoadenine on one strand, 5-hydroxyuracil, 5-formyluracil and a 1 nt gap on the other strand, within 17 bp was built and used to challenge several steps of base excision repair (BER) pathway with human whole-cell extracts and purified repair enzymes as well. We show a hierarchy in the processing of lesions within the MDS, in particular at the base excision step. In the present configuration, efficient excision of 5-hydroxyuracil and low cleavage at 8-oxoguanine prevent DSB formation and generate a short single-stranded region carrying the 8-oxoguanine. On the other hand, rejoining of the 1 nt gap occurs by the short-patch BER pathway, but is slightly retarded by the presence of the oxidized bases. Taken together, our results suggest a hierarchy in the processing of the lesions within the MDS, which prevents the formation of DSB, but would dramatically enhance mutagenesis. They also indicate that the mutagenic (or lethal) consequences of a complex MDS will largely depend on the first event in the processing of the MDS.

INTRODUCTION

Heterogeneous energy deposition by ionizing radiation in DNA results in the formation of multiple lesions within 1–2 helical turns (1,2). Such clustered DNA damage or multiply damaged sites (MDSs) consist of two or more closely spaced oxidized bases, abasic (AP) sites, single-strand breaks (SSBs) distributed on both strands (3). Recent studies showed that X- and γ-rays produce substantial level of clustered DNA damage sites in mammalian cells (4,5). Indeed, clustered DNA damage sites (SSB, oxidized base and abasic clusters) are induced twice as much as double-strand breaks (DSBs). It has been postulated that the probability of clustered lesions formation and their complexity increase with increasing ionization density of radiation (1–3). They are thought to largely contribute to the deleterious effect of ionizing radiation, since they may be difficult to repair. It has been stipulated that repair of clustered DNA lesions may be compromised, possibly leading to the formation of DSB, and thus to lethal events.

Oxidized bases, AP sites and SSB are repaired predominantly by base excision repair (BER), which is a multi-step procedure involving the sequential action of several proteins (6). The excision/incision steps result in a single base gap as a repair intermediate. In higher eukaryotes, there are two alternative BER pathways. The short-patch BER is a DNA polymerase β-dependent pathway and involves the insertion of one nucleotide and rejoining by DNA ligase III/XRCC1. The long-patch BER pathway is dependent on DNA polymerase δ/ε, replication factor C, proliferating cellular nuclear antigen (PCNA), flap endonuclease (FEN1) and DNA ligase I. It implicates a repair patch size of essentially 2–4 nt (up to 10). It is of interest to understand how these processes function when several lesions are clustered at a damaged site.

Recent *in vitro* studies have used oligonucleotides containing two closely opposed radiation-type lesions (oxidized bases, AP sites, SSB) and examined repair efficiency by purified prokaryote and eukaryote BER proteins or cell extracts. Those studies have established that the excision efficiency of a lesion depends on its location relative to the other and on the type of modifications (7–14). The first cleavage event at one of the two opposed oxidized bases is relatively unaffected by the location of the lesions and results in an SSB. The oxidized base on the other strand is then excised only if situated three or more nucleotides away, leading to the formation of a DSB (13). In contrast, a SSB located 1 nt away from an oxidized base on the

*To whom correspondence should be addressed. Tel: +33 1 69 86 71 87; Fax: +33 1 69 86 94 29; Email: Evelyne.Sage@curie.u-psud.fr

opposite strand strongly inhibits base excision with a polarity effect (9–13) and is resealed first (13). In fact, whether or not a double-strand break is formed depends on whether or not the DNA *N*-glycosylase can cleave the base damage opposed to a strand break (14). In *Escherichia coli*, there are indications that two opposed uracil residues located 13–33 bp apart are fully repaired, whereas when situated less than 12 bp apart, they are excised and SSB repair intermediates are converted into DSB (15,16). In addition, it has been demonstrated that in *E.coli*, the mutation frequency of a 8-oxoguanine (oG) is enhanced by the presence of an oG or a uracil situated at 1–5 nt on the opposite strand (17,18).

All *in vitro* and *in vivo* studies to date have used synthetic oligonucleotides designed to contain two radiation-type lesions, one on each strand. Meanwhile, more complex clustered DNA damage has been predicted (1,2,19) and likely represents a fraction of the non-DSB clustered DNA damage revealed in mammalian cells (4,5). In most studies with those synthetic bi-stranded clustered lesions, analysis focused only on one of the two lesions. The results obtained *in vitro* and *in vivo* are somewhat in agreement to some extent. However, to what extent DSBs, resulting from repair intermediates, are produced in cells is still a pending question. In addition, there is no information on the processing of MDS which are more complex than those described above. The presence of more than two lesions at a damaged site may introduce profound changes in the local DNA conformation that may further inhibit interaction with repair enzymes. Also, when different oxidized bases are present at a site, one can ask which one will be recognized and cleaved first in a cell. In line with those questions, we engineered a more complex MDS than those previously studied, which carries four different base lesions and a 1 nt gap. The base damages are 8-oxoguanine (oG), 8-oxoadenine (oA), 5-hydroxyuracil (hU) and 5-formyluracil (fU). They are oxidation products of guanine, adenine, cytosine and thymine, respectively, possibly produced by ionizing radiation (20). Our most complex duplex carries oG and oA on one strand and hU, fU and a 1 nt gap on the other strand, within 17 bp, and opposed lesions are 3 bp apart. With such a construct, we challenged, *in vitro*, different steps of BER using human whole-cell extracts and purified human and bacterial DNA repair enzymes. Our goal was to get insight into the processing of such complex damage, that is likely to be formed at least by densely ionizing radiation [high-linear energy transfer (LET) particles], if not by X- and γ-rays (1). In particular, we asked the question of whether or not excision of modified bases in this context would occur and result in DSB formation. In addition, in order to better understand how such complex MDS is processed and what could be the key elements in repair inhibition if any, MDS of lesser complexities were built and tested. Our results show that there is a hierarchy in the processing of lesions (excision and repair synthesis) within the MDS and in particular in the excision of the distinct base lesions composing the MDS. Interestingly, a DSB can be formed as repair intermediate of an MDS composed of only oxidized bases, whereas it is avoided during the processing of the MDS carrying a 1 nt gap, suggesting that a more complex damaged site could be less deleterious for cells than a damaged site composed out of 2–3 modified bases. Moreover, the repair hierarchy that we observed brings some new insight into the mechanism of BER.

MATERIALS AND METHODS

Substrate oligonucleotides

Unmodified oligonucleotides were purchased from Proligo-France. Oligonucleotides carrying modified bases (Table 1) were synthesized by phosphoramidite chemistry on solid support using an Applied Biosystems Inc. 392 DNA synthesizer, with retention of the 5′ terminal dimethoxytrityl group (trityl-ON mode). The 8-oxoguanine and 8-oxoadenine-containing oligonucleotide (56mer-oG/oA) was prepared using commercially available phosphoramidite monomers of 8-oxo-2′-deoxyguanosine and 8-oxo-2′-deoxyadenosine (Glen Research). The 5-hydroxyuracil (hU)-containing oligonucleotides (56mer-hU and 31mer-hU) were synthesized using a 5-hydroxy-2′-deoxyuridine phosphoramidite building block prepared following a synthetic pathway previously described (21). The 5-formyluracil-containing oligonucleotide (24mer-fU) was prepared using a 5-formyl-2′-deoxyuridine phosphoramidite monomer as reported previously (22). The oG-containing oligonucleotide (56mer-oG/oA) was deprotected in a concentrated ammonia solution of 0.25 M 2-mercaptoethanol for 15 h at 55°C to prevent further oxidation of oG during the deprotection step. The hU- and fU-containing oligonucleotides (56mer-hU, 31mer-hU and 24mer-fU) that have been assembled using phenoxyacetyl protective group for dAdo and dGuo and isobutyryl for dCyt, were deprotected with 50 mM methanolic potassium carbonate for 4 h at room temperature. The oligonucleotides were first purified and detritylated on-line by reverse-phase HPLC (23) and then purified twice by preparative denaturing PAGE. Finally, the DNA oligomers were desalted using NAP-25 Sephadex columns (Amersham Pharmacia Biotech) and then quantified by UV absorption at 260 nm. The purity

Table 1. Oligonucleotides used to generate the DNA substrates

Name	Strand	Damage	Sequence	Position of damage relative to the 5′ end
56-mer A	A	None	5′-CTACACTAgTCTgATCgATgACAgCATgACgTgCTACTgACACTgATCTCgAgCTAC-3′	—
56-mer B	B	None	3′-gATgTgATCAgACTAgCTACTgTCgTACTgCACgATgACTgTACTAgAgCTCgATg-5′	—
56-mer-oG/oA	A	oG/oA	5′-CTACACTAgTCTgATCgATgACAgCAT**oG**ACgTgCT**oA**CTgACATgATCTCgAgCTAC-3′	28,36
56-mer-hU	B	hU	3′-gATgTgATCAgACTAgCTACTgT**hU**gTACTgCACgATgACTgTACTAgAgCTCgATg-5′	33
31-mer-hU	B	hU	3′-gATgTgATCAgACTAgCTACTgT**hU**gTACTgC-5′	8
24-mer-fU	B	fU	3′-CgATgAC**fU**gTACTAgAgCTCgATg-5′	17
31-mer	B	None	3′-gATgTgATCAgACTAgCTACTgTCgTACTgC-5′	—

oG, 8-oxoguanine; OA, 8-oxoadenine; hU, 5-hydroxyuracil; fU, 5-formyluracil.

and integrity of each oligonucleotide were assessed by PAGE analysis after 5′-^{32}P-end-labeling, together with electrospray ionization and MALDI-TOF mass spectrometry measurements.

Proteins

T4 polynucleotide kinase was supplied by Invitrogen Life Technologies. Human DNA polymerase β was purchased from Trevigen. The purified human proteins hOGG1 and APE1, the purified *E.coli* Nth and Fpg proteins were generous gifts from Drs Serge Boiteux and Pablo Radicella (CNRS-CEA, Fontenay-aux-Roses, France). His-tagged human DNA Ligase III and His-tagged XRCC1 were purified as described previously (24) from constructs kindly provided by Dr Keith Caldecott and Sherif El Khamisy (GDSC, Brighton, UK).

Preparation of duplex substrates

Oligonucleotides (Table 1) were assembled to generate the duplex substrates depicted in Figure 1. Oligonucleotides were 5′-^{32}P-end-labeled using T4 polynucleotide kinase and [γ-^{32}P]ATP (4500 Ci/mmol; ICN) according to Sambrook *et al*. (25). Unincorporated nucleotides were removed using a Probe Quant G-50 Micro Column (Amersham Pharmacia Biotech). Labeled oligonucleotides were annealed in 100 mM KCl, 10 mM Tris–HCl, pH 7.8 and 1 mM EDTA, with 1.8-fold molar excess of their respective non-radiolabeled complementary strand, by heating at 95°C for 5 min and slow cooling to room temperature. The annealing efficiency was verified by migration of DNA samples on native 12% polyacrylamide gel.

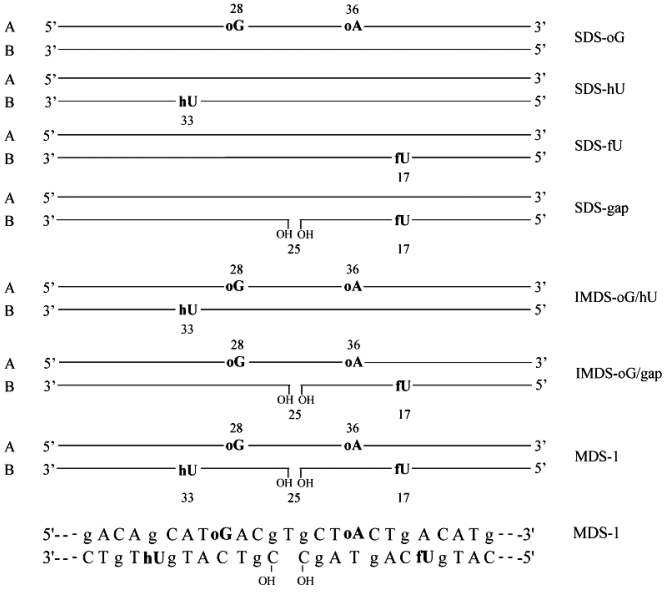

Figure 1. Schematic representation of damaged double-stranded DNA substrates. The oligonucleotides used to generate the DNA substrates are described in Table 1. Duplexes are named as noted on the right-hand side. Substrates called Simply Damaged Site (SDS) carry either oG and oA on strand A, hU or fU, or 1 nt gap and fU on strand B. Substrates named Intermediary Multiply Damaged Site (IMDS) carry oG and oA on strand A and hU, or the 1 nt gap and fU, on strand B. The substrate abbreviated MDS-1 carry oG and oA on strand A, hU, fU and the 1 nt gap on strand B. The position of lesions is relative to the 5′ end. The base damage oA is at 8 nt from oG, hU and fU are at 8 nt from the gap. Opposed lesions are separated by 3 bp. The sequence at the damaged site is given for MDS-1, as example for all the constructs.

Enzymatic cleavage assay

Excision reactions were performed for 30 min at 37°C in a final volume of 10 µl containing labeled double-stranded oligonucleotides (100 fmol), 25 mM Tris–HCl, pH 7.8, 100 mM KCl, 0.1 mM EDTA, 0.4 mg/ml BSA and various amounts of hOGG1, Nth or Fpg proteins, as indicated in the legends of Figures 2, 3 and 4. For cleavage by Nth and Fpg proteins, 1 mM DTT was added to the buffer. The cleavage by APE1 was performed as described previously (26). Following phenol/chloroform extraction, samples were denatured for 5 min at 95°C in denaturing stop solution (94% formamide, 0.1% bromophenol blue, 0.1% xylene cyanol and 10 mM EDTA, pH 8) and loaded onto a 12% denaturing polyacrylamide gel containing 7 M urea and 10% formamide in TBE (89 mM Tris–HCl, 89 mM boric acid and 2 mM EDTA, pH 8.3). The gels were run at 1500 V for 2 h at room temperature. To assess DSB formation, non-denaturing stop solution (75% glycerol, 0.25% bromophenol blue, 0.25% xylene cyanol) was added to the samples which were then submitted to migration on a native 12% polyacrylamide gel in TBE buffer for 180 min at 1000 V. The reaction products were visualized and quantified using a Molecular Dynamics Storm 840 PhosphorImager and ImageQuant software (Molecular Dynamics). The cleavage efficiency was expressed as the percentage of the amount of labeled cleaved molecules to the total amount of labeled (cleaved plus uncleaved) molecules in a lane.

BER assay

The repair reactions were carried out in an appropriate incubation buffer that allows all proteins to be active. Nevertheless, the cleavage efficiency of hOGG1 was reduced in such a buffer. Reaction mixtures (20 µl) contained 100 fmol of labeled double-stranded oligonucleotides, 40 mM Tris–HCl pH 7.6, 100 mM KCl, 1 mM $MgCl_2$, 20 µM of each dNTP, 1 mM ATP and 0.4 mg/ml BSA, plus various combinations of purified enzymes as indicated in the legends to Figure 6 and Figure 2S of the Supplementary Material. The reactions were stopped by heating 10 min at 65°C and then, processed as described above.

Preparation of whole-cell extracts

Transformed human fibroblasts MRC5-V1 (a gift from Dr A. Sarasin, CNRS/IGR, Villejuif France), a cell line which is not sensitive to ionizing radiation, was used to prepare whole-cell extracts. Cells were cultured in DMEM supplemented with 10% fetal calf serum. Exponentially growing cells (1×10^7) were harvested by centrifugation, washed three times with cold PBS and suspended in 200 µl lysis buffer (20 mM Tris–HCl, pH 8.0, 250 mM NaCl, 1 mM EDTA, 20% glycerol and protease inhibitor cocktail from Roche-Applied Science at the concentration recommended by the manufacturer). The cell suspension was sonicated for 10 s on ice, at an amplitude of 9 µm (MSE sonicator). After centrifugation at 4°C for 30 min at 54 900 *g*, the supernatant was collected. Protein concentration was determined by the Bradford colorimetric method and aliquots of cell extracts were conserved at −20°C and used within a month without loss of activity.

Cleavage activity in whole-cell extracts

The assay mixtures (10 µl final volume) contained 200 fmol of labeled double-stranded oligonucleotides and whole-cell extracts (30–40 µg of proteins) in the incubation buffer (20 mM Tris–HCl, pH 8.0, 100 mM NaCl, 0.8 mM EDTA and 8% glycerol), and the reactions were performed at 37°C for the indicated times. The reactions were stopped by the addition of 0.5% SDS, 50 mM EDTA, then incubated with 0.8 µg/µl proteinase K for 1 h at 37°C and, after phenol/chloroform extraction, terminated as described above.

Gap repair by whole-cell extracts

Reactions were performed as for the cleavage activity assay but in a different buffer (40 mM Tris–HCl, pH 7.5, 100 mM NaCl, 0.8 mM EDTA, 4 mM $MgCl_2$, 0.5 mM DTT, 2 mM ATP, 40 mM phosphocreatine, 0.05 mg/µl phosphocreatine kinase, 2 mM NAD, 0.25 mg/µl BSA, and 20 µM of dNTP and ddNTP as specified in the legend to Figure 5) to favor polymerase and ligase activity. The reaction products were analyzed by 20% denaturing PAGE.

RESULTS

We built DNA duplexes carrying multiply damaged sites of increasing complexity. They are depicted in Figure 1. The modified bases, oG, oA, hU and fU are oxidation products of guanine, adenine, cytosine and thymine, respectively. In duplexes they are paired with their normal complementary base, C, T, G and A, respectively. A 1 nt gap harboring 5′- and 3′-OH termini represents a 'non-ligatable' single-strand break. Our most complex duplex (abbreviated MDS-1) carries oG and oA on one strand and hU, fU and a 1 nt gap on the other strand, within 17 bp. Damaged sites of lesser complexities were built to analyze the impact of closely opposed modified bases and of a break on repair efficiency. Two intermediary MDS carry oG and oA on one strand and hU (IMDS-oG/hU) or a 1 nt gap (IMDS-oG/gap) on the other strand. In MDS-1 and IMDS constructs opposed lesions are 3 bp apart. The duplexes named simply damaged sites, SDS-oG, SDS-hU, SDS-fU and SDS-gap served as control substrates for repair of single oG, hU, fU or gap. In fact, SDS-oG carries oG and oA which are 7 nt apart on the same strand and can be considered as individual lesions with respect to the excision by DNA repair enzymes (14). Individually, each lesion included in a damaged site is repaired by BER (6).

Hierarchy in excision process of distinct base lesions within an MDS by whole-cell extracts

In order to get insight into the processing of clustered lesions by human cells, as a first step, we analyzed the excision efficiency of the oxidized bases in MDS-1 by human MRC5-V1 cell extracts. To begin with, the repair capacity of the extracts and the experimental conditions were tested by examining the cleavage of 5′-end-labeled SDS-oG at oG site by various amounts of cell extracts, as a function of time (data not shown). Then, substrates of Figure 1 were ^{32}P-labeled at the 5′ end of the strand carrying the oxidized base to be analyzed for excision, and incubated or not in the presence of cell extracts for 2 h, as defined in preliminary experiments. The excision efficiency was determined from the fraction of cleaved DNA substrate. Considering oG excision, Figure 2A shows that SDS-oG carrying a single oG is efficiently cleaved (lane 2), while the cleavage of the intermediary MDS, IMDS-oG/hU (lane 4) is slightly reduced. A 1.3-fold inhibition, likely due to the presence of the closely opposed hU, was calculated (Figure 2B). In contrast, a strong inhibition of oG cleavage is observed for MDS-1 (Figure 2A, lane 8). Comparative to IMDS-oG/hU, MDS-1 contains a 1 nt gap at 4 nt from oG on the opposite strand that could be responsible for the repair inhibition (10). We tested this hypothesis on the substrate IMDS-oG/gap that contains a 1 nt gap at the same position relative to oG as in MDS-1, but no hU. As expected, we observed a strong excision inhibition relatively to single oG (Figure 2A, lane 6 and B). Only 8% of IMDS-oG/gap and 4% of MDS-1 are cleaved, versus 45% of SDS-oG (Figure 2B). This represents inhibition factors of 6 and 12, respectively. Those observations highlight the relative consequences of hU and a gap located at 4 nt opposite oG, on its excision. (The presence of oA and fU should not play a role since barely repaired, see below.)

However, in the substrate MDS-1, the 1 nt gap which is located at 8 nt 5′ from hU, is not an inhibitory factor for hU excision, nor is the presence of other oxidized base nearby, as demontrated from Figure 2A (lanes 11–16). The substrates containing hU as single lesion (SDS-hU), or within a cluster (IMDS-oG/hU and MDS-1) are equally well excised at hU (Figure 2B). The presence of a closely opposed oG has no effect on hU excision. In addition, the cell extracts are more efficient at excising single hU than single oG (Figure 2B, 65 versus 45% excision, respectively for 2 h incubation, P-value < 0.05 according to Mann–Whitney test). Interestingly, extracts from MRC5V1 cells inactivated for hOGG1 are unable to excise oG in any context (Figure 1S in Supplementary Material), indicating that hOGG1 cannot be significantly substituted by another glycosylase such as NEIL1 (27,28) in our assay. Notably, fU is poorly excised in the MDS-1 (Figure 2A, lane 10), whereas its excision from SDS-fU is about twice as efficient (Figure 2B). This difference may have a conformational origin, or be explained by a competition between hU and fU for the repair proteins. Anyhow, it appears that fU is poorly repaired by cell extracts (<20% excision). In addition, using 3′-end-labeled substrates, we were not able to detect any oA excision by cell extracts (data not shown), suggesting that oA when paired with T is not repaired. This could be due to the fact that hOGG1 cannot recognize and cleave oA paired with T (29).

This first series of data indicates that, in an MDS context, the capacity of base damage to be excised varies tremendously. The excision of hU is as effective as that of isolated hU, whereas oG excision is largely impaired. The gap opposite oG seems to play a major role in this inhibition. As a result, the formation of a DSB as a repair intermediate should be prevented, with respect to the complex MDS.

Double-strand break is possibly formed as a repair intermediate of the MDS composed of oxidized bases, but is avoided in the case of the MDS containing a gap

The excision reaction products were also analyzed on non-denaturating polyacrylamide gel to examine if excision could

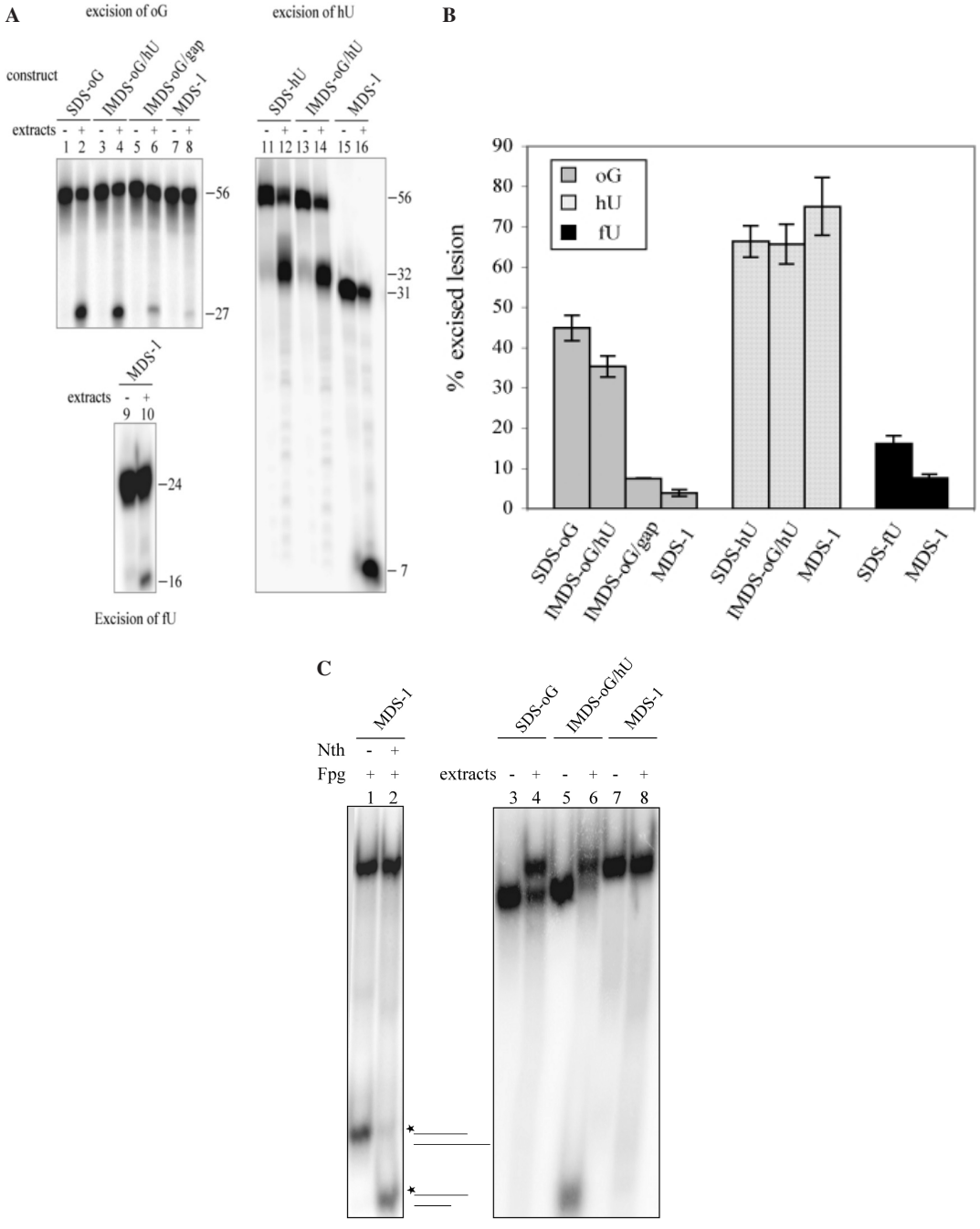

Figure 2. Effect of MDS context on DNA cleavage efficiency at base damages by human whole-cell extracts. Representative denaturing gels (**A**) show cleavage of various substrates at oG (lanes 1–8), fU (lanes 9 and 10) and hU (lanes 11–16): 200 fmol of substrates, 5′-^{32}P-end-labeled on the strand carrying the lesion of interest, were incubated with or without 40 μg of cell extracts for 2 h at 37°C and reaction products were separated by electrophoresis on a 12% denaturing polyacrylamide gel. Graphical representation of the excision efficiencies for each base damage in the different constructs is shown in (**B**) (mean of at least three independent experiments). DSB formation is revealed in (**C**). As above, substrates, 5′-end-labeled on strand bearing oG, were exposed or not to cell extracts (lanes 3–8). In lanes 1 and 2, MDS-1 was incubated 30 min at 37°C with 2.5 nM of Fpg alone or 2.5 nM of Fpg plus 2.5 nM of Nth, respectively. Those two lanes are used as size markers for products generated by cleavage at oG and oG plus hU sites. Reaction products were run on 12% native polyacrylamide gel.

occur on both strands of the same molecule, generating a DSB as repair intermediate. Figure 2C shows the separation of reaction products from substrates 5′-end-labeled on the strand carrying oG and exposed to cell extracts. In order to reveal the presence of products generated by a double excision and thus by the formation of a DSB, MDS-1 was reacted with an excess of Fpg protein (lane 1) or of Fpg plus Nth proteins (lane 2) and cleavage products were used as size markers. (Those proteins excise DNA at oG and hU, respectively.) On native gels, duplexes incised on one strand migrate slower than full-length duplexes (cf. lanes 4, 6, 7 and 8 to lanes 3 and 5 in Figure 2C). Interestingly, for the IMDS-oG/hU substrate incubated with cell extracts, a band migrating as a product of cleavage at oG and hU on the same molecule shows up at the bottom of the gel

(lane 6 to be compared with lane 2). In contrast, for MDS-1 such a band is barely detected (lane 8); in a few cases, we were able to reveal two very faint bands, one corresponding to excision of both oG and hU, the second corresponding to single excision at oG which, in conjunction with the closely opposed gap, generates a DSB. The cleavage products generated by a DSB and revealed on native gels represent not more than 20% of the input for IMDS-oG/hU and 2.5% for MDS-1. This is less than the excision efficiencies observed on denaturing gel (Figure 2B). For IMDS-oG/hU, 45% of the molecules are singly cleaved at hU, 15% are singly cleaved at oG and 20% are incised at both oG and hU. The probability to form a DSB when bistranded base damages such as oG and hU are 3 bp apart is not negligible. Surprisingly, for MDS-1 which carries an interruption in one strand in addition to opposed oG and hU, the excision of oG is largely impaired and consequently, the probability to form a DSB is very low. This suggests that two closely opposed base damages (at least those located 3 bp apart) may be more deleterious for a cell than a more complex MDS harboring several base damages and a non-ligatable gap (or SSB).

Mechanisms of oG cleavage inhibition in MDS-1

One possibility to explain the strong impairment in excision of oG within MDS could be that hOGG1 activity is strongly inhibited. We tested purified hOGG1 activity on SDS-oG, IMDS-oG/hU and MDS-1. Figure 3A shows that hOGG1 is able to excise oG within MDS-1, but to a lower extent relative to single oG. It also reveals that the cleavage of IMDS-oG/hU is slightly inhibited. The inhibition factors calculated from initial slopes are 3 and 1.4, respectively. Structural modifications due to the presence of hU and the gap as well, certainly play a role in the inhibition of hOGG1. In addition, the conformation of the damaged site which carries four oxidized bases within 17 bp and an additional a gap in the middle, may not be favorable for the interaction of hOGG1 with oG and the opposed C in this context.

In fact, the *N*-glycosylase activity of hOGG1 is stimulated by the AP-endonuclease APE1 *in vitro*, and in cells APE1 is likely to be responsible for most of the cleavage of abasic sites left out after the oG excision by the *N*-glycosylase activity of hOGG1 (26,30). Since excision of oG within MDS-1 by hOGG1 is only inhibited by a factor 3, whereas a 12-fold inhibition is observed for cell extracts, we asked if APE1 activity was impaired in the MDS context. The two substrates SDS-oG and MDS-1 were incubated with hOGG1 plus various amounts of purified APE1, and the reaction products were analyzed by PAGE. The increase in oG excision when APE1 is present in the reaction mixture in addition to hOGG1 is very similar for both substrates (factor 2–3, Figure 3B). Considering oG excision, the above observations indicate that hOGG1 is partly inhibited in the MDS context, but not APE1.

APE1 has been demonstrated to excise hU *in vitro* (31). Indeed, Figure 3C reveals that APE1 cleaves relatively well single hU in SDS-hU, and to a lower extent hU within MDS-1. However, we observed a high and similar level of hU excision by cell extracts in any context (Figure 2B). Thus, APE1 is not the principal repair enzyme responsible for hU excision by cell extracts, the proteins hNth, UDG or the NEIL proteins are

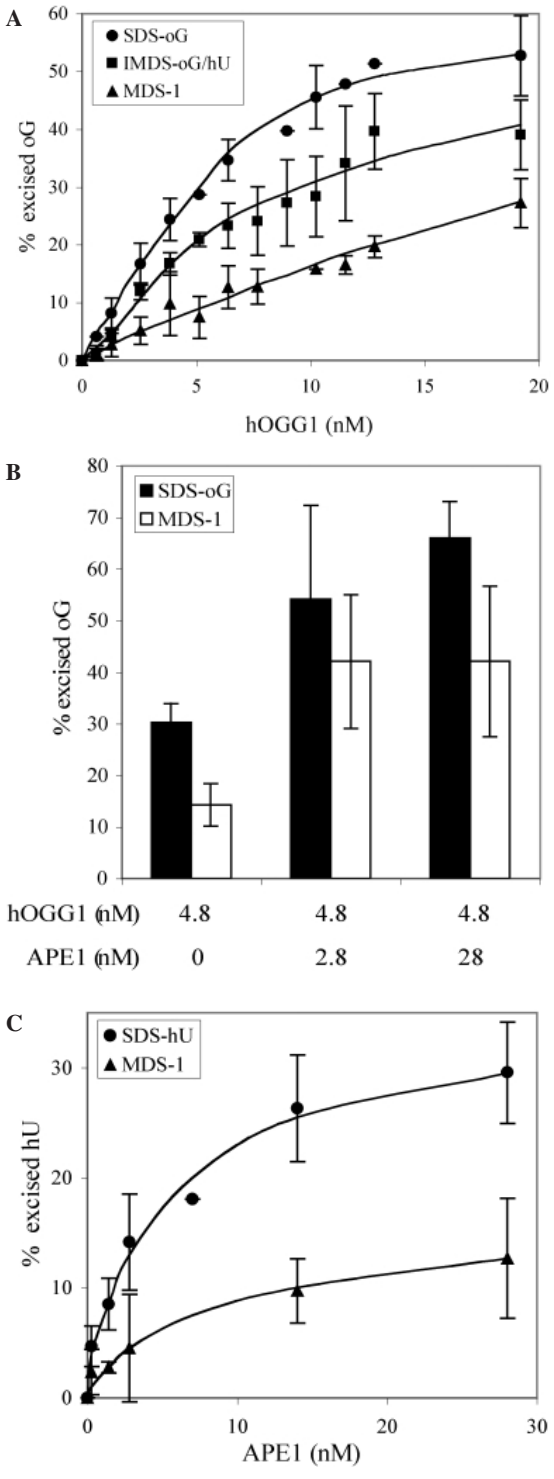

Figure 3. Excision efficiency at oG and hU sites by purified hOGG1 and APE1 proteins: 100 fmol of different substrates, 5′-end-labeled on strand bearing oG (A and B) or hU (C), were incubated for 30 min at 37°C with increasing amount of purified hOGG1 (0–19.2 nM) (A), with 4.8 nM of hOGG1 and 0–28 nM of APE1 (B), or with 0–28 nM APE1 (C). Proteins were eliminated by phenol/chloroform treatment, and DNA samples were subjected to a 12% denaturing polyacrylamide gel. The efficiency of oG excision as a function of hOGG1 concentration is shown in (**A**). The error bars represent the SD from 4–5 independent experiments. The cleavage efficiency at oG by hOGG1 and increasing concentration of APE1 is shown in (**B**). The error bars correspond to the SD of four independent experiments. In (**C**) hU excision by APE1 is shown. SD values of three independent experiments are represented by error bars.

rather involved (32,33). There may be several proteins in charge of hU removal, whereas, only one protein, hOGG1, excises oG, as mentioned above (Figure 1S), which is partly inhibited in the MDS context (Figure 3A).

The above observations lead us to hypothesize that there could be a hierarchy in the kinetics of excision of the different oxidized bases within MDS-1. Using IMDS-oG/hU 5′ end-labeled on both strand in order to detect cleavage at both oG and hU, we performed a kinetic study of excision for short incubation times with cell extracts. Figure 4A shows that hU is excised more efficiently and more rapidly than oG by cell extracts. This suggests that it is the excision of hU, which generates a second break in the strand opposite to oG in MDS-1, that has an inhibitory effect on oG excision by cell extracts, rather than the physical presence of hU. To check the stability of the cleaved MDS-1 substrate carrying two breaks separated by 8 nt on one strand, MDS-1 (and SDS-hU and IMDS-oG/hU as controls) was incubated in the presence of the purified Nth protein from *E.coli*, and the reaction products were separated on native polyacrylamide gel. Interestingly, Figure 4B (lane 6) reveals the presence of an intense band migrating as a very short DNA fragment when MDS-1 is the substrate. In fact, after cleavage of MDS-1 at hU, a 7 nt single-stranded DNA fragment pops out and a 9 nt gap is generated. In those cleaved MDS-1 molecules, oG is thus located on a single-stranded region and cannot be excised by hOGG1, since this enzyme requires a double-stranded substrate and directly interacts with the C residue opposite oG (34).

In fact, in MDS-1 oG excision has a low probability to occur, due to (i) the presence of the 1 nt gap located 3 bp apart on the opposite strand, which slows down hOGG1 activity; (ii) to the fast excision of hU and (iii) to the generation of the 9 nt gap following hU excision. In the rare cases when oG is cleaved first, it does not necessarily prevent hU to be excised but leads to a DSB.

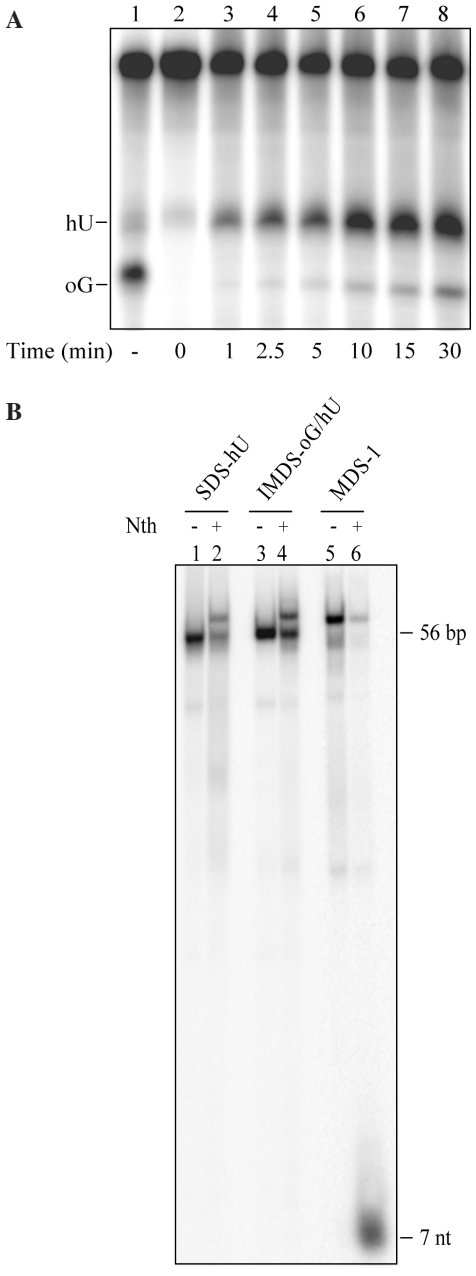

Figure 4. Excision rate of hU by cell extracts is higher than that of oG and generates a 9 nt gap in MDS-1. (**A**) The time course cleavage at oG and hU sites was followed by incubation of IMDS-oG/hU construct (200 fmol) 5′-^{32}P-end-labeled on both strand, for various time periods (0–30 min) with 40 µg of cell extracts (lanes 2–8). The substrate were also subjected to excision at oG by 25 ng of hOGG1 for 30 min at 37°C (lane 1). DNA samples were analyzed on a 12% denaturing polyacrylamide gel. (**B**) SDS–hU (lanes 1 and 2), IMDS-oG/hU (lanes 3 and 4) and MDS-1 (lanes 5 and 6) substrates were 5′-end-labeled on the strand carrying hU and incubated with 3.3 nM of purified Nth proteins for 30 min at 37°C. Samples were subjected to a 12% native PAGE.

Repair of the 1 nt gap and the 9 nt gap left by hU excision

Once we have explored the excision efficiencies of the various oxidized bases contained in the MDS, the repair of the 1 nt gap had to be examined. Indeed, in cells, there exists the possibility that the 1 nt gap is rapidly resealed, before the excision process (13). A further question was that the repair of the 1 nt gap could be impaired in the MDS context, due to the presence of oxidized bases nearby (35) that may introduce an unfavorable local DNA conformation for interaction with a DNA polymerase or ligase. The substrates MDS-1 and control SDS-gap were 5′-end-labeled on the 24mer-fU oligonucleotide (see Table 1 and Figure 1) and incubated in the presence of cell extracts in appropriate buffer. Notably, the buffer for polymerization/ligation differs from that for excision, and in this buffer the excision rate is very low (no more than a few percent) and does not interfere with the resealing to be analyzed. The presence of magnesium also favors nuclease activities, and for long incubation times DNA degradation was observed. The rejoining reaction was thus analyzed for short incubation times (not more than 45 min). Figure 5A and B shows that the 1 nt gap can be efficiently resealed by cell extracts. The addition of 1 nt appears at early times and a large fraction of the molecules are resealed at 30 min in the case of SDS-gap. Rejoining is delayed for MDS-1 (Figure 5B). A limited DNA synthesis through strand displacement is also observed (Figure 5A). To identify if rejoining was processed through short-patch or long-patch BER, dGTP or dTTP were substituted by their dideoxy derivatives, in the reaction mixture. They would be incorporated three and four bases, respectively, downstream from the gap,

by long-patch BER. Anyhow, the rejoining is not inhibited by the presence of ddGTP or ddTTP (Figure 5C, cf. lanes 5 and 6 to lane 3, and lanes 11 and 12 to lane 9), indicating that short-patch BER operates in the repair of the gap. As expected, ddATP is incorporated into the gap and strongly inhibits resealing (Figure 5C, lanes 4 and 10). The DNA polymerase is not retarded by the presence of the base damages since the extent of total polymerization is the same for SDS-gap and MDS-1 substrates (data not shown). This indicates that DNA ligase is retarded, as previously shown (36). Interestingly, after 10 min incubation, some cleavage of hU occurs in the resealed MDS-1 molecules (appearance of a band at 32 nt in Figure 5A). In cells, the resealing would require a kinase to phosphorylate the 5′-OH, a polymerase to insert 1 nt and a ligase to rejoin the ends.

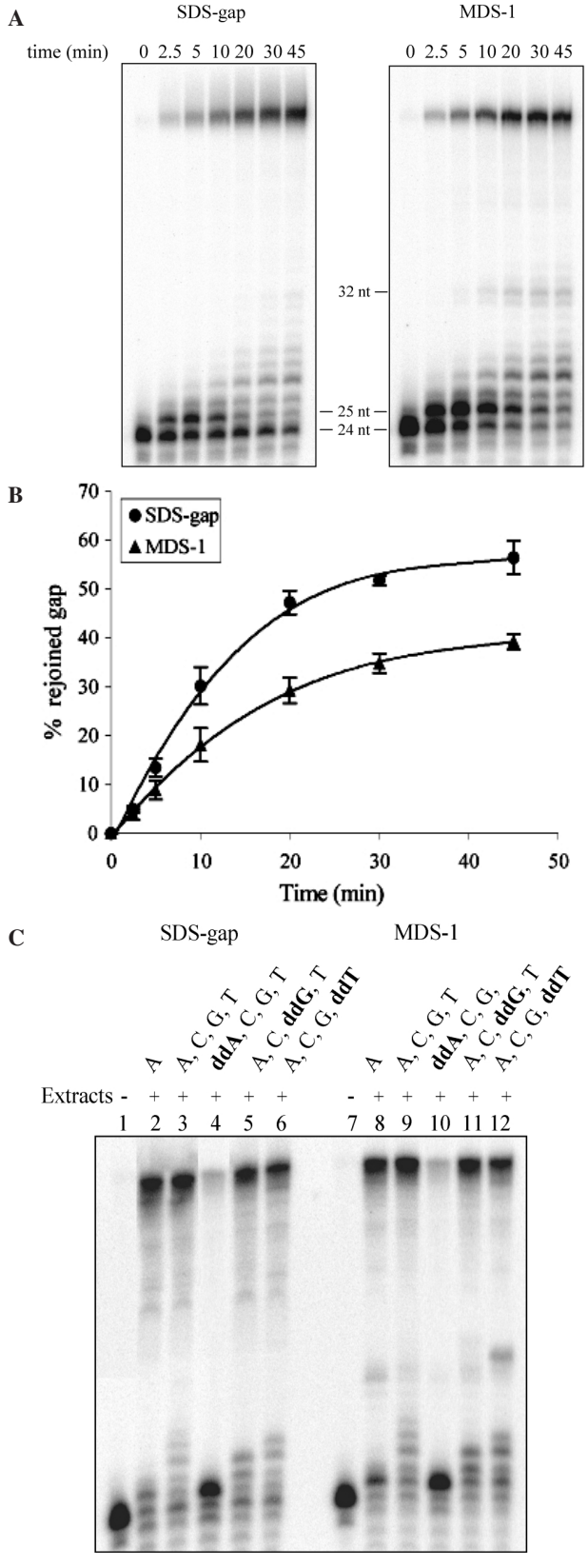

BER and gap repair were reconstituted using 5′-end-labeled 24mer-fU oligonucleotide within MDS-1, commercial human DNA polymerase β (pol β), ligase III/XRCC1 complex and the protein Nth from *E.coli*. Figure 6 shows that pol β is able to efficiently (100%) insert the missing A in the presence of dATP (lane 4), to add C and G, the adjacent bases, after A insertion through a limited strand displacement in the presence of dATP, dCTP and dGTP (lane 5), and to perform strand displacement in the presence of all four dNTPs, but without generating a full-length product (lane 6). When the ligase is added to the reaction mixture, a reduced strand displacement by pol β is observed (lanes 7–9). If Nth is present in the reaction mixture, fU is slightly cleaved (lower band in lanes 2 and 10–12), hU is efficiently excised (not shown in Figure 6, but report to Figure 4C) generating a 9 nt gap. Then, A (lane 10) and ACG (lane 11) are incorporated but ligation cannot take place. In the presence of all 4 dNTPs, DNA synthesis occurs (smear in lane 12) and the gap can be filled, resealed by the ligase, leading to a full-length 56mer product (top band in lane 12). When a phosphate is present at the 5′ extremity of the 1 nt gap (lane 13, MDS is 5′-end-labeled on the 31mer-hU), pol β and ligase efficiently and fully repair the gap by a short patch process, generating a full-length 56mer duplex (lane 13). Whether or not pol β will be used in cells or in cell extracts to reseal the 1 nt gap, will probably depend on the efficiency of a kinase (may be the polynucleotide kinase) to phosphorylate the 5′ end of the gap.

BER was also reconstituted for oG, on substrates SDS-oG, IMDS-oG/hU and MDS-1, which were 5′-end-labeled on the strand carrying oG (see Table 1 and Figure 1), using hOGG1, APE1, pol β and ligase III. In fact, a large part of oG lesions are fully repaired on SDS-oG carrying single oG (see the 56mer full-length repair product in lane 5 of Figure 2S in Supplementary Material). Full DNA repair does not occur in MDS,

Figure 5. Rejoining of a 1 nt gap in the presence or in the absence of closely oxidative base damages. (**A**) SDS-gap or MDS-1 (200 fmol), 5′-end-labeled on strand carrying fU, were incubated for increasing time periods (0–45 min) at 37°C in the presence of 40 μg of cell extracts and 20 μM of each dNTP. The reactions were terminated as in Material and Methods, and samples were analyzed on a 12% denaturing polyacrylamide gel. The time course of rejoining efficiency of the 1 nt gap in SDS-gap or MDS-1 by cell extracts was represented in (**B**). The percentage of rejoined molecules is calculated as the ratio of material migrating as full-length molecules (plus that migrating as 32 nt and corresponding to hU excision from resealed molecules, in the case of MDS-1) to the rest of the material within a lane, including intact 24 nt long molecules and products generated by DNA synthesis. For better accuracy, quantification was performed after separation of reaction products on small polyacrylamide gel (10 cm × 7 cm) leading to only three well-resolved bands, and not from long-run electrophoresis as that in (A). Error bars correspond to SD values of three independent experiments. (**C**) SDS-gap or MDS-1 were treated as described in (A) for 30 min with 20 μM of dNTP and ddNTP as specified in the figure.

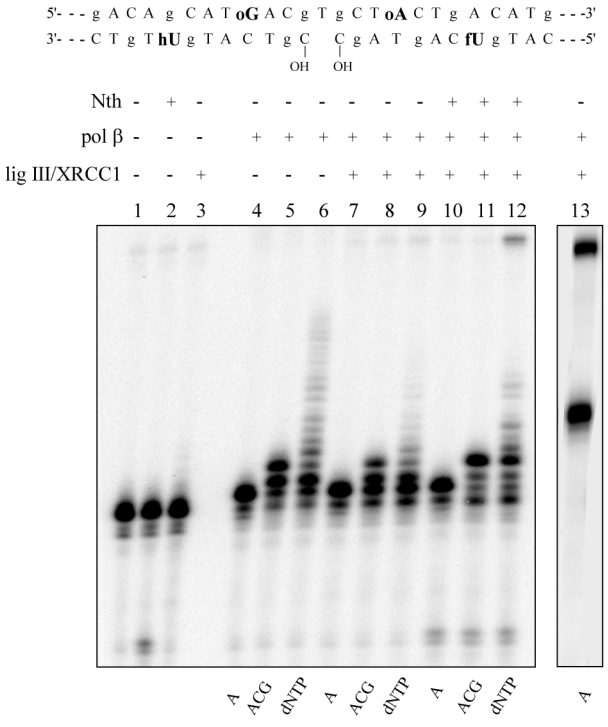

Figure 6. *In vitro* reconstitution of repair at hU and 1 nt gap sites in MDS-1. Part of the sequence of the substrate MDS-1, including the damaged site is represented on the top of the figure. MDS-1 (200 fmol), 5′-^{32}P-end-labeled on the strand carrying fU, was incubated for 30 min at 37°C with Nth (20 nM), pol β (80 nM), DNA ligase III (25 nM), XRCC1 (35 nM) and dATP (lanes 4, 7 and 10), a mixture of dATP, dCTP and dGTP (lanes 5, 8 and 11) or all the dNTPs (lanes 1–3, 6, 9 and 12), as indicated in the figure. In lane 13, MDS-1, ^{32}P-phosphorylated at the 5′ extremity of the strand containing hU, was mixed with pol β, DNA ligase III and dATP (lane 13) as described above. Samples were subjected to 20% denaturing PAGE.

once oG is excised by hOGG1 and the 3′-terminal sugar phosphate removed by APE1 (lanes 9 and 10 in Figure 2S). A DSB is formed, leaving a 5′ overhang that is not filled by pol β.

DISCUSSION

Ionizing radiation produces clustered DNA damage sites that may compromise repair mechanisms in cells and contribute to the deleterious effect of ionizing radiation. We engineered a complex MDS, related to those predicted by Monte Carlo simulation from track structures of ionizing particles. In contrast to the studies published to date, which have mainly analyzed repair or mutagenesis at only one of the two lesions within a synthetic bi-stranded clustered damage site, we were interested in investigating repair of MDS as a whole, i.e. the interplay of damage recognition proteins. We are aware that our construct does not necessarily model all MDS, but the combined use of clustered damage of various complexity with cell extracts and purified repair enzymes allowed to get some clues on the processing of complex MDS. In particular, we present the first evidence that there is a hierarchy in incision rate at the base damages within a complex MDS, and this phenomenon avoids the formation of DSB as repair intermediate. We also show the formation of a short single-stranded region that is potentially mutagenic when carrying a base damage.

All the lesions contained in MDS-1 are repaired by BER, provided that a kinase phosphorylates the 5′ extremity of the 1 nt gap. In human cells, oG is mainly repaired by hOGG1, but it has also been found to be a substrate for hNEIL1 (27). Oxidized purine oA is repaired by hOGG1 when paired with C but not when paired with T (29). Excision of fU could be rather related to uracil-DNA glycosylase hSMUG1 activity (37), but it is also shown with hNTH1 (38,39), thymine-DNA glycosylase hTDG and human methyl-CpG-binding thymine-DNA N-glycosylase (MBD4) (40). In addition, fU can be excised by alkylpurine-DNA-glycosylase II (AlkA) in *E.coli* (41,42). On the other hand, hU has been found to be a rather good substrate for hNTH1, hSMUG1, hNEIL1 and 2 (39,43), and APE1 to a lower extent (31). We were wondering what would be the driving force for the first repair event to be performed when so many damage recognition proteins could interact with the damaged site. A further question was to what extent the observations made using bi-stranded clustered damage sites could apply to a more complex MDS.

One major finding of this study is that in our MDS construct, MDS-1, hU is by far the most efficiently excised lesion by human cell extracts, whereas fU is poorly cleaved, and oG even more poorly excised (Figure 2). We also show (Figure 4A) that hU is the first base damage to be excised from the intermediary MDS (IMDS-oG/hU) which does not contain a gap. In fact, the initial incision rate at hU by cell extracts is higher than that at oG, as isolated lesions (data not shown). Thus, the proteins in charge of oxidized pyrimidine removal have a higher affinity and activity for hU than for fU [as seen for hNTH1 and hNEIL1, (28)], and a higher activity than hOGG1. It appears that *in vitro* hU is a good substrate for hNTH1 and hNEIL1 (28) and is efficiently excised by human cell extracts (our data) and, consequently, in cells, should be efficiently removed from a MDS.

Incision at hU by cell extracts does not seem to be sensitive to the environment, since it is equally efficient for the three substrates tested, SDS-hU carrying a single hU, IMDS-oG/hU and MDS-1 containing other base damages with or without a gap (Figure 2B). Indeed, the presence of oG on the other strand 3 bp apart from hU has no influence on its excision. David-Cordonnier *et al*. (9) reported a 1.5-fold inhibition for incision at another oxidized pyrimidine, dihydrothymine, by Chinese Hamster Ovary (CHO) XRS5 Ku-deficient cell extracts in the presence of a neighboring oG. The cleavage at oG by human cell extracts and by purified hOGG1 as well, is slightly inhibited (1.3–1.4) by the presence of the closely opposed hU (see data on IMDS-oG/hU in Figures 2B and 3A). Similar cleavage inhibitions at oG were observed on bi-stranded clustered lesions composed of oG and uracil or dihydrothymine using nuclear XRS5 cell extracts and purified hOGG1 (10). Therefore, as previously stated, a base damage on the opposite strand has little influence on the excision rate of oG, hU or another oxidative base damage. In contrast, the presence of the 1nt gap 3 bp apart opposite oG has a relatively high inhibitory effect on oG excision by hOGG1, as found by David-Cordonnier *et al*. (10) for their β-δ-SSB, a 1 nt gap terminated by 5′ and 3′ phosphate and located at 3 or 5 nt from oG. A 3-fold inhibition factor was observed in our MDS-1 context, and 4- to 10-fold in their bi-stranded clustered lesion

having the same relative orientation as in our MDS-1, whereas the inhibition was strongly reduced when orientation was reversed. Moreover, with cell extracts, a stronger inhibition of oG excision is observed, i.e. 6-fold inhibition in the context of IMDS-oG/gap and 12-fold for MDS-1 (Figure 2B), in accord with the 10- to 15-fold inhibition obtained on bi-stranded clustered lesion composed of oG and β-δ-SSB 2–4 bp apart, the polarity effect being almost abolished (10). However, in the case of MDS-1, we show that oG excision inhibition is not only due to the presence of the opposed gap but also due to the 9 nt gap left by hU excision. The efficiency of cleavage at oG is particularly sensitive to the local environment, because the activity of hOGG1 in charge of eliminating oG, requires specific contacts of the protein with oG and surrounding bases, in particular with the paired C (34). One can predict that the formation of a SSB as repair intermediate, if not resealed rapidly, will retard the excision of an opposed base damage nearby in an MDS (13). Indeed, this is what is observed in Figure 4A, which shows that in IMDS-oG/hU, incision at oG is delayed by cleavage at hU. A caveat of the above observations is that, depending on the base damages composing a MDS, and in particular on the types of oxidized pyrimidines, the fate and the consequences of the diverse base damages will rely on the first lesion to be cleaved and may vary drastically (see further discussion).

We show that in the IMDS-oG/hU carrying two opposed base damages, simultaneous repair of hU and oG represents one-fourth of the repair events by cell extracts, creating a DSB. In MDS-1, the inhibition of cleavage at oG drastically reduces the probability to form a DSB. *In vivo*, the formation of DSB as repair intermediate of MDS has only been observed for a construct carrying two uracils spaced by ⩽7 nt (16), and it is not clear yet if it would occur for a bi-stranded clustered lesion carrying an oG, since hOGG1 seems more sensitive to the presence of other lesions than proteins involved in excision of modified pyrimidines. On the other hand, in MDS-1, we observed that the cleavage at hU generates in the duplex a short single-stranded region 9 nt long, due to the presence of the 1 nt gap on the same strand. We have strong indications that this also occurs in cells (S. Kozmin and E. Sage, unpublished). Similarly, in a complex MDS composed for example, of several base damages, a short single-stranded region may occur, resulting from simultaneous excision of two base damages situated on the same strand. Such a gap has to be filled by repair synthesis, which may generate a point mutation if a base damage is present on the single-stranded template.

We provide here the first evidence that a gap positioned in a complex MDS can be efficiently resealed by cell extracts. Meanwhile the rejoining is slightly delayed compared to that of an isolated 1 nt gap. A recent *in vitro* study by Lomax *et al*. (36), using simple clustered damage sites comprised of a SSB positioned 1–5 bases 3′ or 5′ of oG on the opposite strand, shows that the repair rate of the SSB is reduced, mainly due to inhibition of the DNA ligase III/XRCC1 complex. The cited work also clearly demonstrates that when the lesions are 5′ to each other, SSB is rather efficiently rejoined by short-patch BER. However, for substrates carrying an oG at 1 or 5 nt on the 3′ side of the SSB on the opposite strand (same orientation as in MDS-1), a very low rejoining efficiency is observed, supposedly by long-patch BER. In contrast, we obtained an efficient resealing, by a short-patch mode. Indeed, addition of 1 nt is seen at early times, and those molecules with the filled gap quickly disappear, whereas rejoined molecules appear (Figure 5A), in spite of a limited strand displacement. Moreover, gap repair is not inhibited by the presence of ddGTP or ddTTP that would be the third or fourth nucleotide, respectively, to be incorporated, whereas it is inhibited by ddATP, the unique nucleotide to be incorporated by short-patch BER (Figure 5C). Interestingly, we also noticed that excision process can occur on resealed molecules shortly after rejoining (Figure 5A). It is reasonable to assume that this phenomenon would have been improbable if the repair of the gap would have proceeded via long-patch BER, for timing reason. Anyhow, we provide evidence using purified human pol β and ligase III/XRCC1 that short-patch BER is efficient for rejoining the break, once phosphorylation has occurred (Figure 6, lane 13). In contrast, the capacity of short-patch BER (with pol β) to fill the 9 nt gap formed by hU excision and rejoin the ends is rather poor (Figure 6, lane 12). This suggests that in cells, long-patch BER involving pol δ/ε may be involved in this process. The observation that hU is excised from rejoined molecules, in addition to the relatively fast resealing of the 1 nt gap obtained with cell extracts is of particular interest. It suggests that in cells a SSB or a small gap in an MDS context may be repaired first, and before base damages are excised. This should particularly occur when an oG is located closely opposed to the gap, since oG excision is delayed and extremely reduced in that situation. Unfortunately, it was not possible to challenge further this hypothesis by *in vitro* assays, as optimal reaction conditions differ for excision and polymerization/ligation.

Our results allow to propose two pathways for the processing of MDS-1 in cells depending on whether or not excision

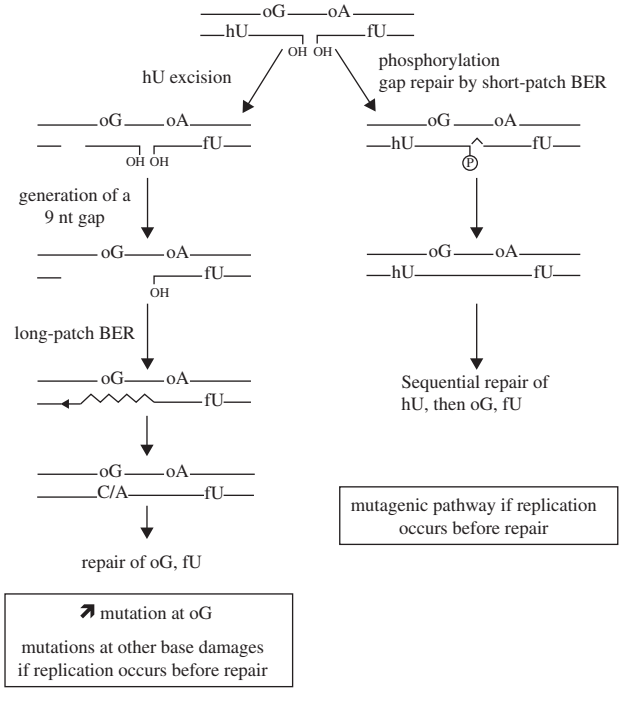

Figure 7. Schematic representation of the proposed processing of MDS-1.

occurs before gap resealing (Figure 7); each mode has different biological consequences. If base excision happens first, hU is the first to be excised, and this creates a 9 nt gap which is probably repaired by long-patch BER. Repair synthesis occurs, therefore, on a damaged template carrying oG and may lead to a mutational event (GC to TA transversion). A simultaneous excision of hU, fU and oG is improbable, and the formation of a DSB is highly unlikely. If the gap is rejoined first, then hU excision will occur afterwards, delaying repair of oG. It is probable that a complete repair of hU takes place before oG is excised (14). However, the probability of forming a DSB *in vivo* in that situation remains to be determined.

More interestingly, using complex MDS, we demonstrate that a strong hierarchy in the excision of base damages present within a clustered DNA damage site exists. Moreover, excision may compete with gap resealing if an SSB is initially present in the damaged site [any complex MDS is likely to contain an SSB (19)]. This repair hierarchy may have several origins. The number, the variety and the structural requirements of repair proteins available for excising each of the base damages may differ. In addition, the conformation of DNA damaged sites may be disturbed, and this would not allow a good interaction with certain repair enzymes (like hOGG1), whereas it would have no effect on others. Structural studies of clustered bi-stranded AP sites showed that the relationship between local DNA conformation at the damaged site and the ability of the lesions to be repaired is not straightforward (44). In accordance with Lin and de los Santos (44), the repair hierarchy implies that the processing of a MDS will largely depend on the nature of the oxidized bases and more specifically, on that of the oxidized pyrimidines, contained in the cluster. Obviously, DNA cleavage at modified base like hU (this study), uracil (16) as well as AP site (45) is fast and very efficient and will be preferred to excision of oG [this study and (45)] or other lesions which are poorer substrates for the BER glycosylases. Other factors like separation between lesions, their orientation relative to each other and the sequence context are likely to play a role (44).

A new feature of the processing of clustered DNA damage sites substantiated by our results is the possibility to generate a short single-stranded fragment as a repair intermediate. In an MDS context, the probability that the polymerase filling the gap meets a base damage is high. This observation also highlights the importance of the interlesion spacing and damage distribution within a cluster. The strong hierarchy in the excision of base damages located in a complex MDS suggests that lesions are still present when repair synthesis and probably also replication occur. This leads to an increased probability to generate mutations, as recently shown for bi-stranded clustered lesions (17,18), and by our own unpublished data. Importantly, our study indicates that the mutagenic (or lethal) consequences of a complex MDS will largely depend on the first event in the processing of the MDS. In the meantime, the stalled repair of clustered lesions results in sequential repair of damages in MDS and minimizes the formation of DSB. This should be more advantageous to cells, since DSB may lead to genetic instability, a possible source of cancer. It appears that multiply damaged sites may rather lead to point mutation than to deletion and may not be as deleterious as initially suspected.

SUPPLEMENTARY MATERIAL

Supplementary Material is available at NAR Online.

ACKNOWLEDGEMENTS

We are grateful to Drs S. Boiteux and P. Radicella (CNRS-CEA, Fontenay-aux-Roses, France) for gift of repair enzymes, and Dr K. Caldecott and Sherif El Khamisy (GDSC, Brighton, UK) for gift of the plasmids carrying human DNA Ligase III and human XRCC1 constructs. We thank Drs P. M. Girard and D. Averbeck (CNRS/Institut Curie, Orsay, France) for stimulating discussions and carefully reading the manuscript. This work was supported by Centre National de la Recherche Scientifique (CNRS), Institut Curie, Centre National d'Etudes Spatiales (CNES), Electricité de France (EDF), Commissariat à l'Energie Atomique. G.E.-H. is recipient of a doctoral fellowship from Ministère de l'Education Nationale, de la Recherche, et de la Technologie. S.E.-M. was recipient of a postdoctoral fellowship from EDF. This work is dedicated to the memory of Professor Claude Hélène. Funding to pay the Open Access publication charges for this article was provided by Institut Curie.

REFERENCES

1. Nikjoo,H., O'Neill,P., Terrissol,M. and Goodhead,D.T. (1994) Modelling of radiation-induced DNA damage: the early physical and chemical event. *Int. J. Radiat. Biol.*, **66**, 453–457.
2. Nikjoo,H., O'Neill,P., Wilson,W.E. and Goodhead,D.T. (2001) Computational approach for determining the spectrum of DNA damage induced by ionizing radiation. *Radiat. Res.*, **156**, 577–583.
3. Ward,J.F. (1988) DNA damage produced by ionizing radiation in mammalian cells: identities, mechanisms of formation, and reparability. *Prog. Nucleic Acid Res. Mol. Biol.*, **35**, 95–125.
4. Gulston,M., Fulford,J., Jenner,T., de Lara,C. and O'Neill,P. (2002) Clustered DNA damage induced by gamma radiation in human fibroblasts (HF19), hamster (V79-4) cells and plasmid DNA is revealed as Fpg and Nth sensitive sites. *Nucleic Acids Res.*, **30**, 3464–3472.
5. Sutherland,B.M., Bennett,P.V., Sutherland,J.C. and Laval,J. (2002) Clustered DNA damages induced by x rays in human cells. *Radiat. Res.*, **157**, 611–616.
6. Slupphaug,G., Kavli,B. and Krokan,H.E. (2003) The interacting pathways for prevention and repair of oxidative DNA damage. *Mutat. Res.*, **531**, 231–251.
7. Chaudhry,M.A. and Weinfeld,M. (1995) The action of *Escherichia coli* endonuclease III on multiply damaged sites in DNA. *J. Mol. Biol.*, **249**, 914–922.
8. Chaudhry,M.A. and Weinfeld,M. (1997) Reactivity of human apurinic/apyrimidinic endonuclease and *Escherichia coli* exonuclease III with bistranded abasic sites in DNA. *J. Biol. Chem.*, **272**, 15650–15655.
9. David-Cordonnier,M.H., Laval,J. and O'Neill,P. (2000) Clustered DNA damage, influence on damage excision by XRS5 nuclear extracts and *Escherichia coli* Nth and Fpg proteins. *J. Biol. Chem.*, **275**, 11865–11873.
10. David-Cordonnier,M.H., Boiteux,S. and O'Neill,P. (2001) Efficiency of excision of 8-oxo-guanine within DNA clustered damage by XRS5 nuclear extracts and purified human OGG1 protein. *Biochemistry*, **40**, 11811–11818.
11. David-Cordonnier,M.H., Cunniffe,S.M., Hickson,I.D. and O'Neill,P. (2002) Efficiency of incision of an AP site within clustered DNA damage by the major human AP endonuclease. *Biochemistry*, **41**, 634–642.
12. Harrison,L., Hatahet,Z., Purmal,A.A. and Wallace,S.S. (1998) Multiply damaged sites in DNA: interactions with *Escherichia coli* endonucleases III and VIII. *Nucleic Acids Res.*, **26**, 932–941.
13. Harrison,L., Hatahet,Z. and Wallace,S.S. (1999) *In vitro* repair of synthetic ionizing radiation-induced multiply damaged DNA sites. *J. Mol. Biol.*, **290**, 667–684.

14. Blaisdell,J.O., Harrison,L. and Wallace,S.S. (2001) Base excision repair processing of radiation-induced clustered DNA lesions. *Radiat. Prot. Dosimetry*, **97**, 25–31.
15. Dianov,G.L., Timchenko,T.V., Sinitsina,O.I., Kuzminov,A.V., Medvedev,O.A. and Salganik,R.I. (1991) Repair of uracil residues closely spaced on the opposite strands of plasmid DNA results in double-strand break and deletion formation. *Mol. Gen. Genet.*, **225**, 448–452.
16. D'Souza,D.I. and Harrison,L. (2003) Repair of clustered uracil DNA damages in *Escherichia coli*. *Nucleic Acids Res.*, **31**, 4573–4581.
17. Malyarchuk,S., Youngblood,R., Landry,A.M., Quillin,E. and Harrison,L. (2003) The mutation frequency of 8-oxo-7,8-dihydroguanine (8-oxodG) situated in a multiply damaged site: comparison of a single and two closely opposed 8-oxodG in *Escherichia coli*. *DNA Repair (Amsterdam)*, **2**, 695–705.
18. Pearson,C.G., Shikazono,N., Thacker,J. and O'Neill,P. (2004) Enhanced mutagenic potential of 8-oxo-7,8-dihydroguanine when present within a clustered DNA damage site. *Nucleic Acids Res.*, **32**, 263–270.
19. Holley,W.R. and Chatterjee,A. (1996) Clusters of DNA induced by ionizing radiation: formation of short DNA fragments. I. Theoretical modeling. *Radiat. Res.*, **145**, 188–199.
20. Cadet,J., Berger,M., Douki,T. and Ravanat,J.L. (1997) Oxidative damage to DNA: formation, measurement, and biological significance. *Rev. Physiol. Biochem. Pharmacol.*, **131**, 1–87.
21. Fujimoto,J., Tran,L. and Sowers,L.C. (1997) Synthesis and cleavage of oligodeoxynucleotides containing a 5-hydroxyuracil residue at a defined site. *Chem. Res. Toxicol.*, **10**, 1254–1258.
22. Berthod,T., Petillot,Y., Guy,A., Cadet,J., Forest,E. and Molko,D. (1996) Synthesis and mass spectrometry analysis of oligonucleotides bearing 5-formyl-2′-deoxyuridine in their structure. *Nucleosides Nucleotides*, **15**, 1287–1305.
23. Romieu,T., Gasparutto,D., Molko,D. and Cadet,J. (1997) A convenient synthesis of 5-hydroxy-2′-deoxycytidine phosphoramidite and its incorporation into oligonucleotides. *Tetrahedron Lett.*, **38**, 7531–7534.
24. Caldecott,K.W., Tucker,J.D., Stanker,L.H. and Thompson,L.H. (1995) Characterization of the XRCC1–DNA ligase III complex *in vitro* and its absence from mutant hamster cells. *Nucleic Acids Res.*, **23**, 4836–4843.
25. Sambrook,J., Fritsch,E.F. and Maniatis,T. (1989) *Molecular Cloning: A Laboratory Manual*. 2nd edn.. Cold Spring Harbor Laboratory, Cold Spring Harbor, NY.
26. Vidal,A.E., Hickson,I.D., Boiteux,S. and Radicella,J.P. (2001) Mechanism of stimulation of the DNA glycosylase activity of hOGG1 by the major human AP endonuclease: bypass of the AP lyase activity step. *Nucleic Acids Res.*, **29**, 1285–1292.
27. Hazra,T.K., Izumi,T., Boldogh,I., Imhoff,B., Kow,Y.W., Jaruga,P., Dizdaroglu,M. and Mitra,S. (2002) Identification and characterization of a human DNA glycosylase for repair of modified bases in oxidatively damaged DNA. *Proc. Natl Acad. Sci. USA*, **99**, 3523–3528.
28. Katafuchi,A., Nakano,T., Masaoka,A., Terato,H., Iwai,S., Hanaoka,F. and Ide,H. (2004) Differential specificity of human and *Escherichia coli* endonuclease III and VIII homologues for oxidative base lesions. *J. Biol. Chem.*, **279**, 14464–14471.
29. Dherin,C., Radicella,J.P., Dizdaroglu,M. and Boiteux,S. (1999) Excision of oxidatively damaged DNA bases by the human alpha-hOgg1 protein and the polymorphic alpha-hOgg1(Ser326Cys) protein which is frequently found in human populations. *Nucleic Acids Res.*, **27**, 4001–4007.
30. Hill,J.W., Hazra,T.K., Izumi,T. and Mitra,S. (2001) Stimulation of human 8-oxoguanine-DNA glycosylase by AP-endonuclease: potential coordination of the initial steps in base excision repair. *Nucleic Acids Res.*, **29**, 430–438.
31. Gros,L., Ishchenko,A.A., Ide,H., Elder,R.H. and Saparbaev,M.K. (2004) The major human AP endonuclease (Ape1) is involved in the nucleotide incision repair pathway. *Nucleic Acids Res.*, **32**, 73–81.
32. Dizdaroglu,M., Karakaya,A., Jaruga,P., Slupphaug,G. and Krokan,H.E. (1996) Novel activities of human uracil DNA *N*-glycosylase for cytosine-derived products of oxidative DNA damage. *Nucleic Acids Res.*, **24**, 418–422.
33. Dizdaroglu,M., Karahalil,B., Senturker,S., Buckley,T.J. and Roldan-Arjona,T. (1999) Excision of products of oxidative DNA base damage by human NTH1 protein. *Biochemistry*, **38**, 243–246.
34. Bruner,S.D., Norman,D.P. and Verdine,G.L. (2000) Structural basis for recognition and repair of the endogenous mutagen 8-oxoguanine in DNA. *Nature*, **403**, 859–866.
35. Budworth,H. and Dianov,G.L. (2003) Mode of inhibition of short-patch base excision repair by thymine glycol within clustered DNA lesions. *J. Biol. Chem.*, **278**, 9378–9381.
36. Lomax,M.E., Cunniffe,S. and O'Neill,P. (2004) 8-OxoG retards the activity of the ligase III/XRCC1 complex during the repair of a single-strand break, when present within a clustered DNA damage site. *DNA Repair (Amsterdam)*, **3**, 289–299.
37. Masaoka,A., Matsubara,M., Hasegawa,R., Tanaka,T., Kurisu,S., Terato,H., Ohyama,Y., Karino,N., Matsuda,A. and Ide,H. (2003) Mammalian 5-formyluracil-DNA glycosylase. 2. Role of SMUG1 uracil-DNA glycosylase in repair of 5-formyluracil and other oxidized and deaminated base lesions. *Biochemistry*, **42**, 5003–5012.
38. Miyabe,I., Zhang,Q.M., Kino,K., Sugiyama,H., Takao,M., Yasui,A. and Yonei,S. (2002) Identification of 5-formyluracil DNA glycosylase activity of human hNTH1 protein. *Nucleic Acids Res.*, **30**, 3443–3448.
39. Ide,H. and Kotera,M. (2004) Human DNA glycosylases involved in the repair of oxidatively damaged DNA. *Biol. Pharm. Bull.*, **27**, 480–485.
40. Liu,P., Burdzy,A. and Sowers,L.C. (2003) Repair of the mutagenic DNA oxidation product, 5-formyluracil. *DNA Repair (Amsterdam)*, **2**, 199–210.
41. Masaoka,A., Terato,H., Kobayashi,M., Honsho,A., Ohyama,Y. and Ide,H. (1999) Enzymatic repair of 5-formyluracil. I. Excision of 5-formyluracil site-specifically incorporated into oligonucleotide substrates by alka protein (*Escherichia coli* 3-methyladenine DNA glycosylase II). *J. Biol. Chem.*, **274**, 25136–25143.
42. Terato,H., Masaoka,A., Kobayashi,M., Fukushima,S., Ohyama,Y., Yoshida,M. and Ide,H. (1999) Enzymatic repair of 5-formyluracil. II. Mismatch formation between 5-formyluracil and guanine during DNA replication and its recognition by two proteins involved in base excision repair (AlkA) and mismatch repair (MutS). *J. Biol. Chem.*, **274**, 25144–25150.
43. Hazra,T.K., Kow,Y.W., Hatahet,Z., Imhoff,B., Boldogh,I., Mokkapati,S.K., Mitra,S. and Izumi,T. (2002) Identification and characterization of a novel human DNA glycosylase for repair of cytosine-derived Lesions. *J. Biol. Chem.*, **277**, 30417–30420.
44. Lin,Z. and de los Santos,C. (2001) NMR characterization of clustered bistrand abasic site lesions: effect of orientation on their solution structure. *J. Mol. Biol.*, **308**, 341–352.
45. Lomax,M.E., Cunniffe,S. and O'Neill,P. (2004) Efficiency of repair of an abasic site within DNA clustered damage sites by mammalian cell nuclear Extracts. *Biochemistry*, **43**, 11017–11026.